High-density amorphous phase of silicon carbide obtained under large plastic shear and high pressure

Valery I. Levitas,[1,*] Yanzhang Ma,[2] Emre Selvi,[2] Jianzhe Wu,[2] and John A. Patten[3]
[1]*Departments of Aerospace Engineering, Mechanical Engineering, and Material Science and Engineering, Iowa State University, Ames, Iowa 50011, USA*
[2]*Department of Mechanical Engineering, Texas Tech University, Lubbock, Texas 79409, USA*
[3]*Department of Manufacturing Engineering, Western Michigan University, Kalamazoo, Michigan 49008, USA*
(Received 20 September 2011; revised manuscript received 4 December 2011; published 29 February 2012)

In situ x-ray diffraction study of the hexagonal 6H SiC under pressure and shear in rotational diamond anvil cell is performed that reveals phase transformation to the new high-density amorphous (hda) phase SiC. In contrast to known low-density amorphous SiC, hda-SiC is promoted by pressure and unstable under pressure release. The critical combination of pressure ∼30 GPa and rotation of an anvil of 2160° that causes disordering is determined.

DOI: 10.1103/PhysRevB.85.054114 PACS number(s): 64.60.−i, 64.70.K−, 46.35.+z

I. INTRODUCTION

Phase transformations (PTs) in SiC under high pressure and shear are of great fundamental and applied interest, including understanding and controlling the behavior of SiC under penetration for armor applications, wear, polishing, cutting, scratching, and indenting, as well as for a ductile machining regime. Our main focus in this paper is on hexagonal 6H SiC; however, because the energy difference between 6H SiC and cubic 3C SiC is small[1] and some similarities in phase behavior are expected, we include 3C SiC in the discussion. A review of PTs in SiC is given in Ref. 2. Experimentally, there has been no report of a high-pressure PT in 6H SiC up to 95 GPa in a diamond anvil cell (DAC), while some new x-ray peaks appeared above 90 GPa.[3] Under shock compression, PT to, most likely, a rock salt structure starts at 100 GPa and completes at 137 GPa.[4] Similarly, 3C SiC transforms to the rock salt structure in DAC ∼100 GPa.[3] Pressure-induced amorphization in SiC was not observed experimentally, in contrast to some molecular dynamic (MD) simulations[5–7] and to amorphization in materials with a similar structure, like ice,[8] Si,[9] silica,[10] and $AlPO_4$[11] (see the review in Ref. 12). The most intriguing problem is related to amorphization of 6H SiC, which was observed in the transmission electron microscopy (TEM) study of chips after ductile machining.[13] It was stated that the chips were amorphous, although the typical amorphous halo ring in TEM was lacking. Amorphous SiC was observed by Raman study in a hardness impression of 3C and 2H SiC but was not found in the TEM study.[2,14] In the MD study[15] on 3C SiC, amorphization was observed in the region a few nanometers in size under a flat, square indenter with a side of 3 nm. It was identified by analysis of the radial distribution function and bond angle distribution and caused by coalescence of dislocation loops. Under a spherical indenter, only dislocation activity without PT was obtained in MD simulations.[16] Partial disordering was also obtained in MD simulations of scratching of 3C SiC.[17] Scratch hardnesses (scratching force over the contact area, excluding the chip) were 89 and 332 GPa in different directions. Usually, the amorphous phase appears under the indenter during back transformation from high pressure during unloading.[2] However, no direct evidence of PTs to a high-pressure phase were observed in SiC during postprocessing of nanoindents. Amorphous SiC can also be obtained by ion implantation,[18] and its density is 14% lower than that for crystalline SiC before annealing and 7% lower than that for crystalline SiC after annealing; this indicates the existence of different forms of amorphous SiC. Amorphous SiC obtained in MD simulations from melt also had a lower density than the crystalline phase.[16] While the existence of various amorphous phases of SiC among existing forms cannot be excluded (similar to polyamorphism in ice,[8,19] Si,[9,20] and carbon[21]), low-density amorphous (lda) SiC has a lower density than crystalline SiC. Then, direct pressure-induced amorphization to lda-SiC is impossible because of its density is lower and its enthalpy is higher[16] than those for crystalline SiC. The only known possibility is that shear stresses and large plastic strains cause amorphization. The goal of the current paper is to study SiC under compression and shear in a rotational diamond anvil cell (RDAC) to determine possible crystal–crystal and crystal–amorphous PTs and define the amorphization path and conditions. The experimental setup and methods are described elsewhere.[22–24] The superposition of large plastic shear on high pressure in an RDAC significantly reduces the PT pressure (by a factor of 2–5), may lead to promoting the formation of novel phases, substitutes reversible PT (RPT) with irreversible PT, and leads to amorphous and nanostructured materials.[25] However, SiC has never been studied under pressure and shear in RDAC. Thus, PT to the new high-density amorphous (hda) phase SiC is revealed, which (in contrast to lda-SiC) is promoted by pressure and is unstable under pressure release. Pressure–shear conditions for the appearance of hda-SiC are determined.

II. EXPERIMENTAL STUDY

In situ x-ray diffraction studies have been carried out on SiC in an RDAC using the synchrotron radiation facilities in the National Synchrotron Light Source at Brookhaven National Laboratory and the Cornell High Energy Synchrotron Source at Cornell University. Two methods were used in the measurements: the energy-dispersive method and the angle-dispersive method (wavelength of 0.4958 nm). SiC produced by CoorsTek (trade name SC 30) represented by 800-grit powder that was more than 99% pure 6H SiC (without the

sintering agent) was used in these experiments. SiC was loaded in gaskets made of stainless steel without pressure-transmitting media. The sample was first compressed to a given pressure, and the rotation of the anvil was performed under constant axial force. Anvils with 400-μm diamond culets were used. Pressure distributions were measured using the fluorescence of fine ruby grains of $\sim$1 μm distributed over the sample surface. The gasket was initially preindented to 20 GPa and $\sim$40 μm thickness. For all samples, rotation of an anvil at a constant axial force led to a significant increase in pressure in the sample. This is possible if initial pressure in the gasket is approximately homogeneous after compression and then redistributed with a large pressure gradient during plastic flow caused by the rotation. By changing the initial sample thickness and axial force, various pressure–shear loading programs can be fully explored.[22–24]

Sample 1. With the energy-dispersive method, the measurements were performed after compression up to 0.72, 6.82, and 11.15 GPa at the sample center. After rotation of an anvil by 180°, pressure at the center increased to 23.3 GPa; after additional rotation by 180°, pressure at the center increased to 32.22 GPa. As shown in Fig. 1, the rotation significantly changes the relative intensity of the diffraction peaks but does not change the number of diffraction lines. The refinement of the diffraction patterns to the 6H SiC structure shows a good fit within the experimental error. Thus, such a loading program generates defects and may cause some texture but does not cause PT.

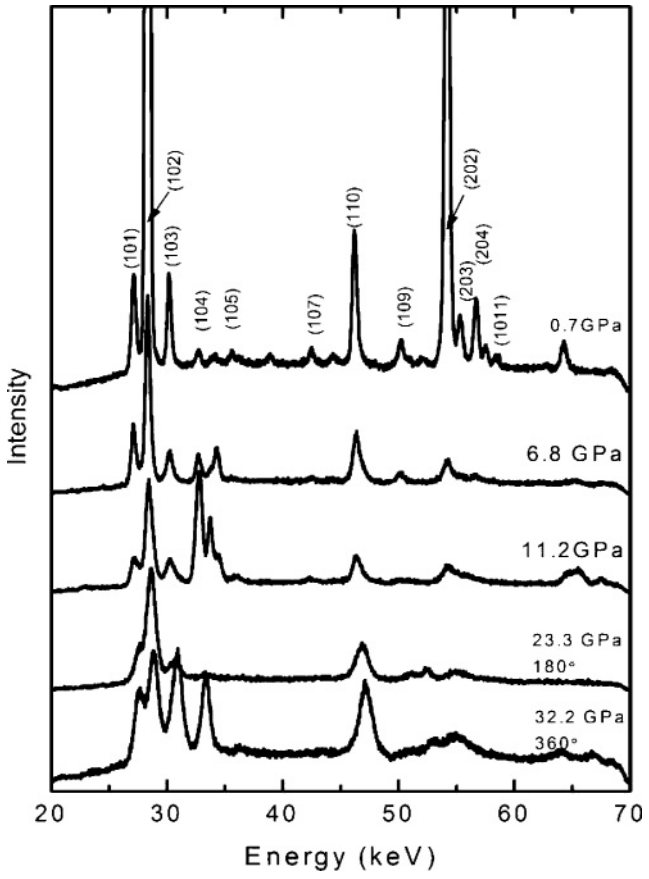

FIG. 1. X-ray diffraction pattern for sample 1. Rotation angles in degrees and pressure at the center of the sample after rotation are shown near the two lower curves; pressure after compression is shown near the three upper curves. The top pattern marks the index of the peaks of SiC. All other peaks can be indexed into ruby.

Sample 2. To promote amorphization, rotations were performed starting at lower pressure and with a much larger angle. Fig. 2(a) shows the pattern change after each compression–shear process. Fig. 2(b) demonstrates the change of x-ray diffraction pattern after 2360° of rotation at initial pressure of 3.3 GPa, leading to pressure of $\sim$30 GPa. Thus, a total rotation of 1080° at pressure up to 30 GPa (with most of the rotation $\sim$30 GPa) did not cause complete disordering, because some peaks are still visible. However, after the additional 1080° of rotation resulting in combined rotation of 2160°, all peaks practically disappear, which means that *amorphization took place*. Additional rotation by 200° did not lead to any further changes. Surprisingly, when the sample was quenched to the ambient pressure, the peaks reappeared [Figs. 2(a) and 2(c)], which indicates that the *amorphous phase recrystallizes back* to the initial 6H SiC state. The peaks are broad, which is probably because the recrystallized phase has a nanograined structure.

Sample 3. Starting rotation at 3.1 GPa, the diffraction spectra (at the center and 25 μm from the center of the sample) and pressure distribution were recorded after each rotation increment (Figs. 3 and 4). After 1230° and 1630° angular rotations, the pressure distribution abruptly changed from being slightly heterogeneous to having a very large pressure gradient, which corresponds to initiation of more intense radial flow. After this stage, the anvil could not be further rotated. According to Fig. 3, there are no indications of amorphization, even when 25 μm from the center with rotation of 1630° and pressure as low as 13 GPa.

Clearly, the rotation angle qualitatively characterizes the magnitude of plastic strain but is not a physical parameter. According to our theory of strain-induced PTs,[25] local accumulated plastic strain plays the role of a timelike parameter in the kinetic equation. However, our simulations[26,27] show that it is distributed very heterogeneously even without PTs and is not a measurable parameter. Figure 5 determines the width of diffraction peaks (full width half maximum) Δ versus the rotation angle at the center of a sample and the point 25 μm from the center. The width Δ is a measure of heterogeneity of the stress state, in our case mostly resulting from internal nonhydrostatic stresses because of various defects generated during plastic deformation (e.g., dislocations and grain boundaries), which promote strain-induced PTs. Because Δ for each peak is a growing function of the rotation angle, it can be considered a physical measure of plastic strain that can be measured *in situ*. It is logical that for the same rotation angle, the width Δ for all peaks is larger at the point 25 μm from the center than at the center, because an average shear strain is proportional to the radius. Operating with several peaks yields more reliable information. If we assume that the main reason for the peak broadening is defect accumulation, then according to Fig. 5, defect accumulation consists of two major steps: very fast accumulation at small rotations (up to 30°) and much slower accumulation at larger rotations. Disappearance or sharp diversion of all peaks can be used to detect and quantify amorphization. Because peaks

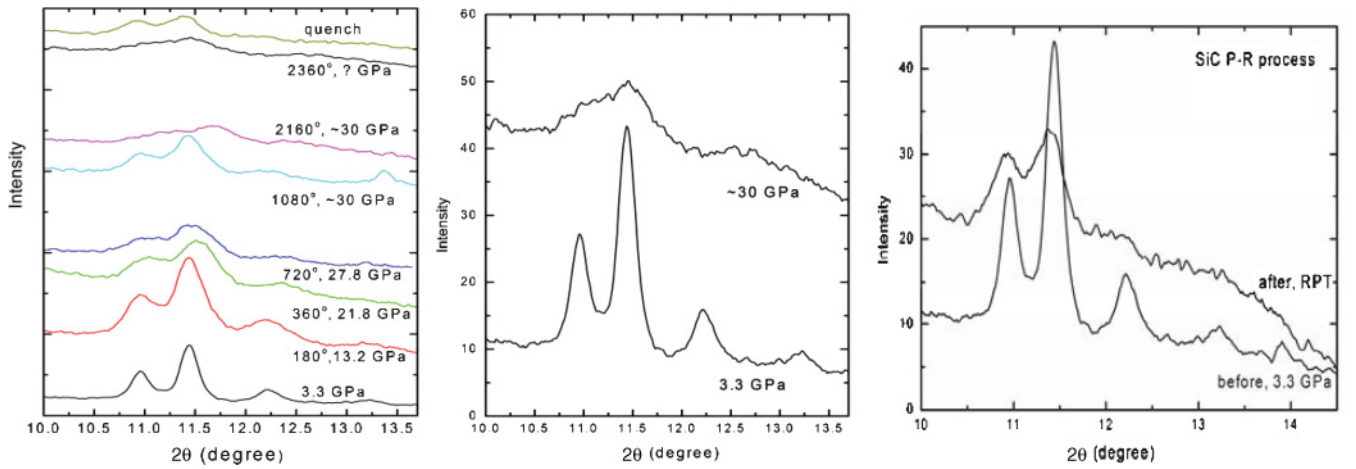

FIG. 2. (Color online) *In situ* x-ray diffraction patterns for sample 2. (a) X-ray diffraction patterns after compression and shear processes (marked near curves) and quenching to ambient pressure. The pressure at 2360° is not measurable. (b) X-ray diffraction patterns after rotation by 2360° at initial compression to 3.3 GPa, leading to disordering of SiC. (c) Comparison of x-ray diffraction patterns after compression to 3.3 GPa and after quenching to ambient pressure after all operations. The disordered phase transforms back to the crystalline 6H phase after pressure release (P-R).

characterize internal stresses and PT is caused by total stresses (i.e., external and internal), an amorphization criterion can in principle be formulated as a combination of measured local pressure and width Δ. Also, to exclude the heterogeneity of internal stresses under hydrostatic loading, it would be more precise to reduce the width Δ by the corresponding value obtained under the same hydrostatic pressure. This research direction will be pursued in future studies.

III. DISCUSSION

The only PT observed in the pressure range up to 32 GPa and under very large shear is to a disordered phase of SiC. There were no indications of PTs to other SiC polymorphs, e.g., C SiC or rock salt structure, which may be expected under large shear. There are three possibilities in interpretation of the obtained results:

(1) The obtained phase is highly disordered nanocrystalline but is not an amorphous phase, because some broad peaks can be distinguished in Fig. 2(b).

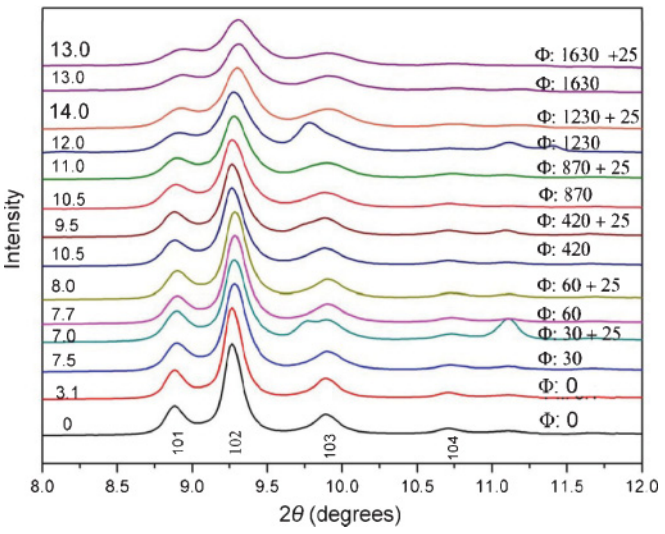

FIG. 3. (Color online) X-ray diffraction pattern of SiC for sample 3. Numbers above patterns on the left are corresponding pressures. Numbers on the right are rotation angles and offset positions to the rotation center.

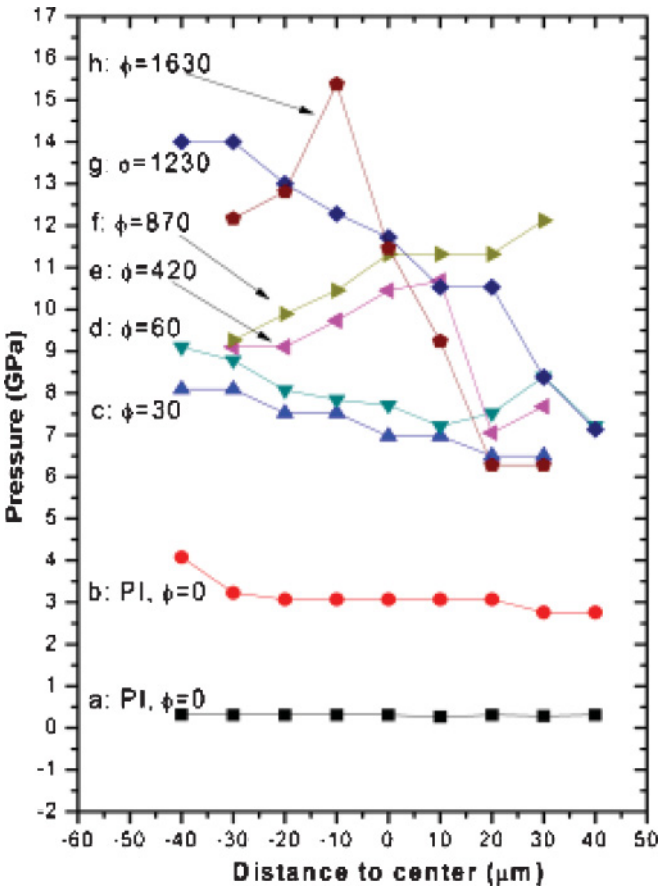

FIG. 4. (Color online) Pressure distributions after each operation for sample 3. Pressure increase (PI) marks an increase in load.

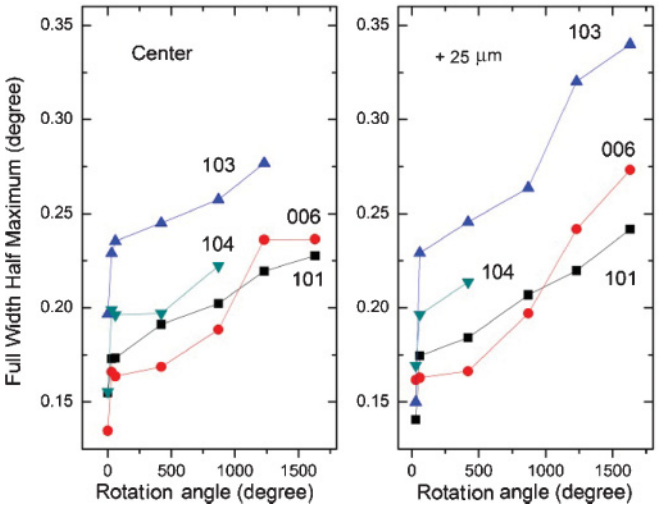

FIG. 5. (Color online) Effect of shear on the width of diffraction peaks of SiC for sample 3. Data from Fig. 3 are used. (a) The center of a sample. (b) The point 25 μm from the center.

(2) The obtained phase is the known lda-SiC.

(3) A new amorphous phase was obtained, which is referred to as the hda-SiC.

These options are summarized here, along with justification that the most probable interpretation corresponds to hda-SiC.

In the first possibility, simulations demonstrated that plastic deformation in an RDAC is very heterogeneous along the sample height before,[26,27] during, and after PT.[28–30] Plastic strain localizes near the contact surfaces, where it can exceed by a factor of 3 to 10 the plastic strain near the plane of symmetry of a sample. At the same time, pressure does not vary significantly throughout the thickness of a sample. Because disordering occurs as some critical combination of pressure and plastic strain, it should start near the contact surfaces and propagate to the plane of symmetry. However, x-ray patterns are averaged over the sample thickness. Even if a major part of a sample has amorphized, some peaks from the remaining crystalline phase are observable. Thus, we detect the disordered phase not when it appears but when the volume fraction of the crystalline phase along the sample height becomes small and is not represented in x-ray spectra. Consequently, remaining broad peaks in Fig. 2(b) cannot be considered as contradictions to the existence of an amorphous phase.

Torsion under pressure is one of the main methods of producing nanocrystalline materials.[31] However, at room temperature, a nanostructure does not disappear after pressure release, which allows us to study and use these materials under ambient pressure. But in our experiments peaks reappeared, which is typical for reverse PT rather than the disappearance of the nanocrystalline structure. This is why we concluded that our results were consistent with amorphization under high pressure and plastic straining followed by recrystallization after pressure release rather than with formation of a nanocrystalline structure.

In the second option, although we obtained amorphous SiC under high pressure and shear, it cannot be the amorphous lda-SiC that is studied in Refs. 2, 13, 15, 17, and 18, used in engineering applications,[32] and can be obtained by the quenching of melt. Indeed, PT to lda-SiC should be suppressed by pressure because of the larger specific volume of lda-SiC: if it appeared under high pressure, it should not transform back under pressure release because the driving force for recrystallization reduces with reduced pressure. We might expect that even if lda-SiC did not appear during plastic deformation under high pressure, it may nucleate at defects produced by plastic deformation after rapid pressure release. This was probably the case for amorphization during machining.[2] In contrast, our hda-SiC appeared only at pressure as high as 30 GPa. The lda-SiC is metastable at ambient pressure and even at nanoindentation of initially amorphous SiC[33]; hda-SiC is unstable at ambient pressure and recrystallizes to 6H SiC.

Finally, for these findings to be noncontradictory, it is necessary to assume that the specific volume of hda-SiC is smaller than that of 6H SiC. Then, both high pressures promoting disordering and pressure release leading to recrystallization are in agreement with thermodynamics. This is the main reason that the obtained phase is designated hda-SiC. Both of these facts imply that amorphization represents a PT (rather than defect accumulation and the mechanism of plastic deformation because of suppressed dislocation activity) and that amorphization has a thermodynamic nature; i.e., the hda-SiC phase has lower Gibbs energy under high pressure than the crystalline phase with defects generated by plastic deformation. As the material undergoes such large plastic strain before disordering, its dislocation activity is not suppressed under such a pressure.

In MD simulations,[15,17] amorphization occurred in regions a few nanometers in size because of suppressed dislocation activity; in experiments,[13] it occurred in 100-nm chips. In the experiments described in this paper, disordering occurred in the sample that was 10 μm thick (the thickness of the sample after all operations) and underwent a plastic deformation two orders of magnitude larger than in previous studies.[13,15,17]

According to the theory,[25] strain-induced PTs occur at stress concentrations produced by defects generated during plastic deformation (e.g., dislocation pileups and grain boundaries). Because the scale in work reported herein is much larger than that reported elsewhere,[13,15,17] the dislocation pileup can contain a much greater number n of dislocations. Because stress concentration is proportional to n, pressure at the tip of defects can be on the order of 100 GPa, and shear stresses can reach the ideal maximum material strength. Thus, plastic shear is not equivalent to just the superposition of shear stress on the hydrostatic pressure. This leads to a drastic increase in the pressure in a small region near the tip of the defect. For SiC, pressure reduces ideal shear strength.[34] One of the main possible theoretical mechanisms of pressure-induced amorphization in SiC is related to shear instability of the crystal lattice.[5–7] Application of large shear stresses should promote this instability. Because pressure causes amorphization in MD simulations,[5–7] the product cannot be lda-SiC, and we assume that it is hda-SiC obtained in the current work. Thus, when plastic shear is large enough to generate a sufficient number of dislocations and when local pressure and shear stresses are high enough, the lattice loses its stability, and a PT to hda-SiC occurs. The transformed region cannot grow far from the defect tip because of the reduction of stress concentrations. Thus, rotation increments are necessary to generate new defects and

hda-SiC PT at their tips. Alternatively, large plastic shear can lead to nanocrystalline material with disordered grain boundaries and large stresses near boundaries,[31] an increase in shear can lead to an increase in concentration of grain boundaries and their complete amorphization—i.e., to hda-SiC (as in Ref. 35 for lda-SiC)—and crystalline peaks will not be visible in x-ray patterns.

IV. CONCLUSIONS

In situ x-ray diffraction studies reveal PT of 6H SiC to the new amorphous hda-SiC phase under pressure and shear in an RDAC. This is the first report on a polyamorphism in SiC, which was previously found in ice,[8,19] Si,[9,20] and carbon.[21] In contrast to a-SiC, hda-SiC is promoted by pressure and is unstable under unloading. (1) Shear at 23 GPa, even when pressure reached 32 GPa after the total 360° (sample 1); (2) shear by a total of 1080°, leading to 30 GPa (sample 2); and (3) shear by a total of 1630°, leading to 16.5 GPa (sample 3), are not sufficient for the disordering of SiC. Total rotations of 2160° and 2360° at pressure of ∼30 GPa completes disordering, which determines critical conditions for amorphization. Such an RPT, which is not detectable by TEM, may significantly affect the mechanical properties of SiC under extreme loading. No other PTs are observed under the described loading program. The relationship between the width of the diffraction peaks Δ and the rotation angle allows interpretation of the results in terms of the measurable physical parameter Δ and hypothetically defines two stages of defect accumulation. In the future, research will be attempted to narrow the critical conditions for generation of hda-SiC, to transform the entire sample into an amorphous state, and to arrest the hda-SiC by further plastic deformation.[25]

ACKNOWLEDGMENTS

US Army Research Office (Contract No. W911NF-09-1-0001), Iowa State University, and Texas Tech University support for this research is gratefully acknowledged. Discussions with M. Kramer and R. Ott of Ames Laboratory, as well as comments of anonymous reviewers, are appreciated.

*vlevitas@iastate.edu

[1] K. J. Chang and M. L. Cohen, Phys. Rev. B **35**, 8196 (1987).
[2] Y. Gogotsi and V. Domnich, in *High Pressure Surface Science and Engineering*, edited by Y. Gogotsi and V. Domnich (Institute of Physics Publishing, Bristol, UK, 2004), p. 443.
[3] M. Yoshida, A. Onodera, M. Ueno, K. Takemura, and O. Shimomura, Phys. Rev. B **48**, 10587 (1993).
[4] T. Sekine and T. Kobayashi, Phys. Rev. B **55**, 8034 (1997).
[5] K. Mizushima, M. Tang, and S. Yip, J. Alloys Compd. **279**, 70 (1998).
[6] M. Tang and S. Yip, Phys. Rev. Lett. **75**, 2738 (1995).
[7] S. Yip, J. Li, M. Tang, and J. Wang, Mater. Sci. Eng. A **317**, 236 (2001).
[8] O. Mishima, L. D. Calvert, and E. Whalley, Nature **310**, 393 (1984).
[9] M. F. McMillan, M. Wilson, D. Daisenberger, and D. Machon, Nat. Mater. **4**, 680 (2005).
[10] R. J. Hemley, A. P. Jephcoat, H. K. Mao, L. C. Ming, and M. H. Manghnani, Nature **334**, 52 (1988).
[11] M. B. Kruger and R. Jeanloz, Science **249**, 647 (1990).
[12] E. G. Ponyatovsky and I. O. Barkalov, Mater. Sci. Rep. **8**, 147 (1992).
[13] J. Patten, W. Gao, and K. Yasuto, J. Manuf. Sci. Eng. **127**, 522 (2005).
[14] T. F. Page, L. Rester, and S. V. Hainsworth, in *Fundamentals of Nanoindention and Nanotribology*, edited by N. R. Moody, W. W. Gerberich, N. Burnham, and S. P. Barker (Materials Research Society, University of Michigan, 1998), Vol. 522, p. 113.
[15] I. Szlufarska, R. K. Kalia, A. Nakano, and P. Vashishta, Phys. Rev. B **71**, 174113 (2005).
[16] M. Mishra and I. Szlufarska, Acta Mater. **57**, 6156 (2009).
[17] A. Noreyan and J. G. Amar, Wear **265**, 965 (2008).
[18] V. Heera and F. Prokert, Appl. Phys. Lett. **70**, 3531 (1997).
[19] R. J. Nelmes, J. S. Loveday, T. Strässle, C. Bull, M. Guthrie, G. Hamel, and S. Klotz, Nat. Phys. **2**, 414 (2006).
[20] B. Haberl, A. C. Y. Liu, J. E. Bradby, S. Ruffell, J. S. Williams, and P. Munroe, Phys. Rev. B **79**, 155209 (2009).
[21] D. R. McKenzie, D. Muller, and B. A. Pailthorpe, Phys. Rev. Lett. **67**, 773 (1991).
[22] V. I. Levitas, Y. Ma, J. Hashemi, M. Holtz, and N. Guven, J. Chem. Phys. **125**, 044507 (2006).
[23] Y. Ma, E. Selvi, V. I. Levitas, and J. Hashemi, J. Phys. Condens. Matter **18**, 1075 (2006).
[24] V. I. Levitas, Y. Ma, and J. Hashemi, Appl. Phys. Lett. **86**, 071912 (2005).
[25] V. I. Levitas, Phys. Rev. B **70**, 184118 (2004).
[26] V. I. Levitas and O. M. Zarechnyy, Appl. Phys. Lett. **91**, 141919 (2007).
[27] V. Levitas and O. Zarechnyy, Int. J. High Press. Res. **30**, 653 (2010).
[28] V. I. Levitas and O. M. Zarechnyy, EPL **88**, 16004 (2009).
[29] V. I. Levitas and O. M. Zarechnyy, Phys. Rev. B **82**, 174123 (2010).
[30] V. I. Levitas and O. M. Zarechnyy, Phys. Rev. B **82**, 174124 (2010).
[31] R. Z. Valiev, R. K. Islamgaliev, and I. V. Alexandrov, Prog. Mater. Sci. **45**, 103 (2000).
[32] M. Le Contellec, J. Richard, A. Guivarc'h, E. Ligeon, and J. Fontenille, Thin Solid Films **58**, 407 (1979).
[33] I. Szlufarska, R. K. Kalia, A. Nakano, and P. Vashishta, J. Appl. Phys. **102**, 023509 (2007).
[34] Y. Umeno, Y. Kinoshita, and T. Kitamura, Model. Simulat. Mater. Sci. Eng. **15**, 27 (2007).
[35] I. Szlufarska, A. Nakano, and P. Vashishta, Science **309**, 911 (2005).